Mesoscale Simulation of Grain Growth

David Kinderlehrer, Jeehyun Lee, Irene Livshits and Shlomo Ta'asan

WILEY-VCH Verlag Berlin GmbH
September 4, 2003

0.1 Introduction

The mesoscale simulation of grain growth consists in resolving a large coupled system of nonlinear evolution equations with appropriate boundary conditions which represents a network of interfaces. We present here an approach based on a dissipation principle and flexible enough to exploit the energy and mobility functions derived from recent experiments. Our objective is to simulate with sufficient accuracy to predict texture and at a sufficient scale to yield meaningful statistics. Since, generally, the result of such a simulation consists of the statistics it provides, we are led to the companion issue of coarse graining in mesoscale simulations. We seek to understand what statistics are reliable and how we may interrogate the dynamics of their distribution functions. There are many challenges to the successful execution of this program, from the algorithmic level where we are confronted with a highly nonlinear coupled system with many toplological events or critical events, to the coarse grain level. For reasons of space, we defer discussion of this latter subject to a future work.

A number of collateral references are listed in the references. We would like to take this opportunity to thank A. D. Rollett and G. Rohrer and also G. Leoni, C. Liu, and P. Yu for their help. Supported by the MRSEC program of the NSF under award DMR 0079996 and NSF DMS 0072194, NSF DMS 9805582, NSF DMS 0305794 and the DoE Computational Materials Science Network

Here we are concerned with the mesoscale simulation of large networks of grains or interfaces in two and three dimensions. The evolution is governed by the Mullins Equation of curvature driven growth. These equations, discussed below, are a system of evolution parabolic partial differential equations for each grain boundary curve, in two dimensions, or facet, in three dimensions. Grain boundaries meet, typically, at triple junctions, in two dimensions, or on triple lines, in three dimensions, where an additional boundary condition is required. We enforce the Herring Condition, a force balance, and below we show that it is the natural boundary condition for the Mullins Equation in equilibrium. Other boundary conditions are admissible but the Herring Condition is the simplest. The resulting system is then dissipative for the energy and the evolution can be viewed as a modified steepest descent for the total grain boundary energy. In addition, we must treat certain critical events. During evolution, a grain boundary or a grain may shrink and disappear. This creates unstable multiple junctions which split into triple junctions which we treat in a way that results in maximum energy reduction.

Our first objective is to review the Mullins Equation and to establish that the Herring Condition is its natural boundary condition. The two dimensional version of this has been presented in [17]. Consider a network of grains with facets which meet in triple lines. The most direct way to proceed is to begin with three facets represented as graphs over an $x = (x_1, x_2)$ plane meeting along a triple line Γ,

$$\begin{array}{ll} S^{(i)} : z = u^{(i)}(x), & x \in \Omega_+, i = 1, 2 \\ S^{(3)} : z = u^{(3)}(x), & x \in \Omega_- \\ u^{(1)} = u^{(2)} = u^{(3)} & on \quad \Gamma' \end{array} \tag{1}$$

where Γ' denotes the projection of Γ onto the x-plane. Consider first a single facet, say

$$S : z = u(x), \quad x \in \Omega (= \Omega_+)$$

The energy density of the facet S is given by

$$\begin{aligned} &\sigma(n), \quad n = \frac{1}{W}(-p_1, -p_2, 1), \quad \textit{the normal to } S \\ &p_i = \frac{\partial u}{\partial x_i}\,, \quad W = \sqrt{1+|p|^2} \end{aligned} \tag{2}$$

σ is positively homogeneous of degree 0, and thus $\nabla_n \sigma \cdot n = 0$. The energy of S is

$$E = \int_\Omega \sigma(n) W dx \tag{3}$$

and equilibrium is determined by

$$\delta E = 0 \tag{4}$$

We give a brief derivation of the equilibrium equation which enables us to verify that the discrete version determined in the next section is an approximation of it. Let η be a test variation with compact support in Ω and

$$\begin{aligned} &z = u + \epsilon\eta, \\ &E_\epsilon = \textstyle\int_\Omega \sigma(n_\epsilon) W_\epsilon dx, \\ &n_\epsilon = \frac{1}{W_\epsilon}(-(p_1+\epsilon q_1), -(p_2+\epsilon q_2), 1), \quad q = \nabla\eta \\ &W_\epsilon = \sqrt{1+|p+\epsilon q|^2} \end{aligned}$$

and

$$\frac{dn_\epsilon}{d\epsilon} = -\frac{1}{W}(1 - n\otimes n)q \quad \frac{dW_\epsilon}{d\epsilon} = \frac{p\cdot q}{W} \quad . \tag{5}$$

This leads to

$$\begin{aligned} \frac{d}{d\epsilon}E_\epsilon &= \int_\Omega \left(\nabla_n\sigma(n)\frac{dn_\epsilon}{d\epsilon}W_\epsilon + \sigma\frac{dW_\epsilon}{d\epsilon}\right) dx \\ &= \int_\Omega \left(\nabla_n\sigma(n)\cdot(-q_1,-q_2,0) + \sigma\frac{p\cdot q}{W}\right) dx \\ &= \int_\Omega div\left(\nabla_n\sigma(n) - \sigma\frac{p}{W}\right)\eta\, dx \end{aligned} \tag{6}$$

So equilibrium is determined by the equation

$$div(\nabla_n\sigma(n) - \sigma\frac{p}{W}) = 0 \qquad in \quad \Omega \tag{7}$$

If

$$S_t : z = u(x,t), \quad x\in\Omega, \quad t>0,$$

is an evolving family of interfaces, its normal velocity is given by

$$v_n = n\cdot\frac{\partial}{\partial t}(x_1, x_2, u) = \frac{1}{W}\frac{\partial u}{\partial t}$$

and the governing equation of motion is the Mullins Equation

$$v_n = \frac{1}{W}\frac{\partial u}{\partial t} = -\mu\, div\left(\nabla_n \sigma(n) - \sigma\frac{p}{W}\right) \quad in\ \Omega, \quad t > 0, \tag{8}$$

where μ is a given mobility function.

To understand the boundary condition on the triple line Γ, we must consider complete three dimensional variations $\zeta = (\zeta_1, \zeta_2, \zeta_3)$ of the surface S, rather than simply vertical ones. Here it is useful to introduce the variations separately as

$$\begin{aligned} x &= \xi \\ u &= z + \epsilon\, \zeta_3 \end{aligned} \tag{9}$$

$$\begin{aligned} x_1 &= \xi_1 + \epsilon\, \zeta_1 \\ x_2 &= \xi_2 \\ u &= z \end{aligned} \tag{10}$$

$$\begin{aligned} x_1 &= \xi_1 \\ x_2 &= \xi_2 + \epsilon\, \zeta_2 \\ u &= z \end{aligned} \tag{11}$$

The last two are variations of domain. We caution that although at first glance this procedure appears to permit three different equilibrium equations, they are, in fact, all the same. The result of the computation is a linear functional of ζ given by, with the abbreviation $F = \sigma W$,

$$L(\zeta) = \int_\Omega \zeta \cdot n\ div\ F_p\, W dx + \int_{\Gamma'} \zeta \cdot T(\nu)\, ds \tag{12}$$

where $T(\nu)$ is the linear form on the normal ν of Γ' given by

$$T(\nu) = \begin{pmatrix} F - p_1 F_{p_1} & -p_1 F_{p_2} \\ -p_2 F_{p_1} & F - p_2 F_{p_2} \\ F_{p_1} & F_{p_2} \end{pmatrix} \nu$$

Recalling that $F = \sigma W$, we can decompose $T(\nu)$ as

$$\begin{aligned} T(\nu) &= \frac{\sigma}{W}\begin{pmatrix} 1 + (p_2)^2 & -p_1 p_2 \\ -p_1 p_2 & 1 + (p_1)^2 \\ p_1 & p_2 \end{pmatrix} \nu \ + \ W \begin{pmatrix} -p_1\sigma_{p_1} & -p_1\sigma_{p_2} \\ -p_2\sigma_{p_1} & -p_2\sigma_{p_2} \\ \sigma_{p_1} & \sigma_{p_2} \end{pmatrix} \nu \\ &= \ \sigma\, T_{iso}(\nu) + T_{an}(\nu), \end{aligned}$$

with T_{iso} the isotropic term corresponding to the T which arises for constant surface energy and T_{an} containing the torques. Let $l = (l_1, l_2, l_3) = (-\nu_2, -\nu_1, -\nu_2 p_1 + \nu_1 p_2)$ denote the tangent direction to the curve Γ. We then find that

$$T_{iso} = \sigma n \times l \quad \text{and} \quad T_{an} = W^2(\sigma_{p_1}\nu_1 + \sigma_{p_2}\nu_2)n \tag{13}$$

To clarify equilibrium we return to the system of three surfaces. Let $\zeta^{(i)}$ denote the variation (vector) of surface $S^{(i)}$. The variation is the sum of three versions of (9). Let us make

the convention that n^1 and n^2 point upward and n^3 points downward. Then we find

$$\sum_{i=1}^{2}\left(\int_{\Omega_+}\zeta^{(i)}\cdot n^{(i)}\ div\ F_p^{(i)}\ W^{(i)}dx\right)+\int_{\Omega_-}\zeta^{(3)}\cdot n^{(3)}\ div\ F_p^{(3)}\ W^{(3)}dx$$
$$+\quad\sum_{i=1}^{3}\left(\int_{\Gamma'}\zeta\cdot T^{(i)}(\nu^{(i)})\ ds\right)=0 \tag{14}$$
$$subject\ to\quad \zeta^{(1)}=\zeta^{(2)}=\zeta^{(3)}\ on\ \Gamma'$$

Thus, in addition to the equilibrium of equations given by (7), we obtain the natural boundary condition, which is the Herring Condition,

$$T^{(1)}(\nu^{(1)})+T^{(2)}(\nu^{(2)})+T^{(3)}(\nu^{(3)})=0 \tag{15}$$

For example, in the case where σ is independent of n, we immediately verify that

$$n^{(1)}+n^{(2)}+n^{(3)}=0,$$

namely, that the surfaces meet at angles of $2\pi/3$.

We shall discuss simulating a large network of evolving surfaces subject to (8) with (15). An important property of this system is that, in the absence of critical events, it is dissipative. To check this, observe that the total energy of the network is given by

$$E(t)=\sum_S\int_\Omega\sigma^S(\nu)dS \tag{16}$$

and computing dE/dt corresponds to setting $\zeta=-\partial u/\partial t$ in the first variation. After substituting (8), we obtain that

$$\frac{dE}{dt}=-\sum_S\int_\Omega\frac{1}{\mu^S}(v_n)^2dS+\sum_\Gamma\int_\Gamma v\cdot\sum_\Gamma Tds \tag{17}$$

Thus, when (15) holds, the integrals over the triple lines vanish and

$$\frac{dE}{dt}=-\sum_S\int_\Omega\frac{1}{\mu^S}(v_n)^2dS\le 0$$

0.2 Discretization

We proceed by presenting the discretization of the equations above using a dissipation principle. Given a triangulation $T=\beta$ of a surface S consisting of traingles β , the discrete energy of S is

$$E=\sum_{\beta\in T}\sigma(n_\beta)A_\beta$$

where n_β is the normal to β and A_β is the area of β.
The energy rate of change resulting from a motion of the vertices of the triangles $\beta\in T$ is

$$\frac{dE}{dt}=\sum_{\beta\in T}\left[\ \nabla_n\sigma(n_\beta)\cdot\frac{dn_\beta}{dt}A_\beta+\sigma(n_\beta)\frac{dA_\beta}{dt}\ \right] \tag{18}$$

Let x_i, x_j and x_k be three nodes of β, and $W = (x_j - x_i) \times (x_k - x_i)$. Then we may write

$$\begin{aligned} & n_\beta = \frac{W}{|W|} \text{ and } A_\beta = |W| \\ & \frac{dn_\beta}{dt}|W| + n_\beta \frac{d|W|}{dt} = \frac{dW}{dt} \\ & \frac{dA_\beta}{dt} = \frac{W}{|W|} \cdot \frac{dW}{dt} \end{aligned} \tag{19}$$

Combining (18) and (19) yields

$$\begin{aligned} \frac{dE}{dt} &= \sum_{\beta \in T} \left[\nabla_n \sigma(n_\beta) \cdot (\frac{dW}{dt} - n_\beta \frac{d|W|}{dt}) + \sigma(n_\beta) \frac{W}{|W|} \cdot \frac{dW}{dt} \right] \\ &= \sum_{\beta \in T} \left[(\nabla_n \sigma(n_\beta) + \sigma(n_\beta) n_\beta) \cdot \frac{dW}{dt} \right] \end{aligned} \tag{20}$$

We compute

$$\frac{dW}{dt} = \left(\frac{dx_j}{dt} - \frac{dx_i}{dt} \right) \times (x_k - x_i) + (x_j - x_i) \times \left(\frac{dx_k}{dt} - \frac{dx_i}{dt} \right)$$

and let $H = \nabla_n \sigma_\beta + \sigma_\beta n_\beta$, then

$$\begin{aligned} \frac{dE}{dt} &= \sum_{\beta \in T} \left[H \cdot \left(\left(\frac{dx_j}{dt} - \frac{dx_i}{dt} \right) \times (x_k - x_i) \right) - H \cdot \left(\left(\frac{dx_k}{dt} - \frac{dx_i}{dt} \right) \times (x_j - x_i) \right) \right] \\ &= \sum_{\beta \in T} \left[- \left(\frac{dx_j}{dt} - \frac{dx_i}{dt} \right) \cdot (H \times (x_k - x_i)) + \left(\frac{dx_k}{dt} - \frac{dx_i}{dt} \right) \cdot (H \times (x_j - x_i)) \right] \\ &= \sum_{\beta \in T} \left[H \times (x_k - x_j) \cdot \frac{dx_i}{dt} + H \times (x_i - x_k) \cdot \frac{dx_j}{dt} + H \times (x_j - x_i) \cdot \frac{dx_k}{dt} \right] \end{aligned}$$

Introducing notation $t_{\beta i} = x_k - x_j$, this is reduced to

$$\begin{aligned} \frac{dE}{dt} &= \sum_{\beta \in T} \sum_{x_l \in \beta} \left\langle H \times t_{\beta l} \, , \frac{dx_l}{dt} \right\rangle \\ &= \sum_{\beta \in T} \sum_{x_l \in \beta} \left\langle H \times (n_\beta \times m_{\beta l}) |t_{\beta l}| \, , \frac{dx_l}{dt} \right\rangle \\ &= \sum_{\beta \in T} \sum_{x_l \in \beta} \left\langle (H \cdot m_{\beta l}) n_\beta |t_{\beta l}| - (H \cdot n_\beta) m_{\beta l} |t_{\beta l}| \, , \frac{dx_l}{dt} \right\rangle \end{aligned}$$

We obtain

$$\frac{dE}{dt} = \sum_{x_l \in Nodes} \sum_{\beta_l} \left\langle (\nabla_n \sigma(n_\beta) \cdot m_{\beta l}) n_\beta |t_{\beta l}| - \sigma(n_\beta) m_{\beta l} |t_{\beta l}| \, , \frac{dx_l}{dt} \right\rangle \tag{21}$$

where β_l is the set of triangles in T invloving the node x_l.

This gives the discrete form of the evolution equations,

$$v_n = -\sum_{\beta_l} [\, (\nabla_n \sigma(n_\beta) \cdot m_{\beta l}) |t_{\beta l}| - (\sigma(n_\beta) m_{\beta l} \cdot n_\beta) |t_{\beta l}| \,] \tag{22}$$

which clearly are dissipative.

To see the relation between these expression and the continous version given in the previous section, we use the tangential divergence theorem, and the tangential Green's theorems,

$$\begin{aligned} \int_\Omega div_\Omega u \, d\Omega &= \int_\Omega u \cdot n\kappa \, d\Omega + \int_{\partial\Omega} u \cdot m \, d\Gamma \\ \int_\Omega \nabla_\Omega \varphi \, d\Omega &= \int_\Omega \varphi n\kappa \, d\Omega + \int_{\partial\Omega} \varphi m \, d\Gamma \end{aligned}$$

where u, n, m are vectors and φ is a scalar. This gives,

$$v_n = -div(\nabla_n \sigma(n) + \sigma n)$$

which agrees with formula (8).

0.3 Numerical Implementation

We describe here the details of our numerical scheme. The basic objects involved in three dimensional simulation are grain boundaries, triple lines and grains, (in two dimension we use triple junctions, and grain boundaries). Grain boundaries and triple lines are discretized and evolved in our simulation. Unlike several other methods, in this method we do not discretize grains; they are determined by the triple lines and grain boundaries. Our discretization of surfaces and triple lines uses second order finite difference approximations, with either explicit or implicit time stepping. The time evolution of nodal points is done in two steps. First, grain boundaries are moved by Mullins Equation, and then triple lines are moved to enforce the Herring Condition. As grain boundaries and triple lines move, critical events must be considered to reflect actual changes in the physical topology, such as collapse and disappearance of individual grains, as well as to avoid element collapse in the simulation.

Grain boundaries are defined by a collection of triangles consisting of three nodal points and evolution is done by moving the nodal points according to (22). In the case of isotropy, $\sigma = 1$, it reduces to

$$v_n = \sum_{\beta_l} R_{\beta_l} \tag{23}$$

where β_l has three nodal points x_l, x_j, x_k and

$$R_{\beta_l} = \frac{1}{4A_\beta} [\, -|x_k - x_j|^2 \, x_l + (x_k - x_j) \cdot (x_k - x_l) \, x_j + (x_j - x_k) \cdot (x_j - x_l) \, x_k \,]$$

With an explicit time scheme, this gives the discrete evolution equation

$$x_l(t + \tau) = x_l(t) + \tau \sum_{\beta_l} R_{\beta_l}(t) \tag{24}$$

where τ denotes the time step.
Now, we consider an implicit time scheme to accelerate the computation. Let N denote the number of nodal points of the grain boundary S and

$$\mathbf{x}(t) = [\, x_1(t),\, x_2(t), \cdots,\, x_N(t)\,]^T$$

Define an operator

$$L\mathbf{x}(t) = \left[\sum_{\beta_1} R_{\beta_1}(t),\, \sum_{\beta_2} R_{\beta_2}(t), \cdots,\, \sum_{\beta_N} R_{\beta_N}(t) \right]^T$$

Then an implicit method requires solving the system of equations

$$\left(I - \frac{\tau}{2}L\right)\, \mathbf{x}(t+\tau) = \left(I + \frac{\tau}{2}L\right)\, \mathbf{x}(t) \tag{25}$$

and it is approximated by applying Gauss-Seidel iterations.

Triple lines are defined by a set of nodal points and the Herring Condition is imposed on these points. The Herring Condition at a nodal point x_l is given by

$$\sum_{\beta_l} R_{\beta_l} = 0 \tag{26}$$

where β_l is the set of triangles in T invloving the node x_l. And it is also approximated by Gauss-Seidel iterations.

Critical Events

During evolution, three types of critical events occur in three dimensions: loss of grains, loss of facets and loss of triple lines. The critical events are detected by monitoring the size and the rate of changes of topological components (i.e. grains, facets and triple lines). Components that are shrinking fast compared to their size trigger critical events, unless they are growing. This scheme follows Kuprat [23]

`Loss of grains:` In this event a neghboring grain, denoted by wg, will absorb the small target grain tg. The choice of wg is made as follows. We first pick the smallest facet of the target grain tg. Then consider all the facets of the grain tg that have a common triple line with that small facet. We pick from these facets the one with the largest area. It has two grains on its two sides. One of them is our target grain. The other is the neighboring grain wg that will absorb.

`Loss of facet:` Implementation of this event involves two processes, 1) creation of a new volume, 2) loss of grain event. Creation of a new grain is done by growing the target facet, denoted by ts, in the normal direction, into a new grain ng. The new grain is built using a partial volume of two grains meeting at the target facet ts. A loss of grain event is then performed using all neighboring grains except the two which contributed to growing the new grain.

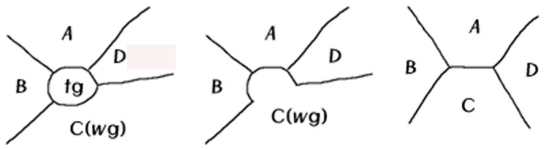

Figure 1: 1.the small grain tg is the target grain for removal; 2.tg is assigned to wg; 3.boundaries have straightened due to the curvature driven motion

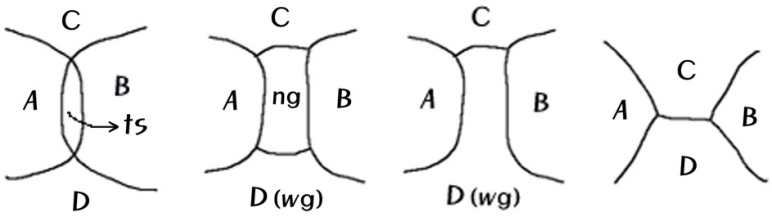

Figure 2: 1.the small facet ts is detected for removal; 2.a new volume ng is created; 3.ng is merged into wg due to the loss of grain; 4.curvature driven motion have straightened the boundaries

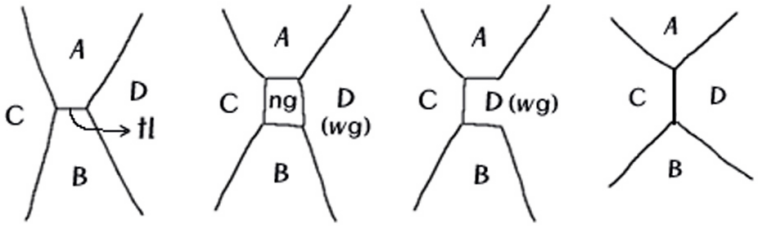

Figure 3: 1.the short horizontal triple line tl is subject to removal; 2.a new volume ng is built; 3.ng is merged into wg due to the loss of grain; 4.curvature driven motion have straightened the boundaries

`Loss of triple line:` Basically, the same idea as in loss of facet applies to the loss of triple line. We build a new volume ng around the target triple line tl using a partial volume from the three grains meeting at that line. We then perform a loss of grain event using all neighboring grains except those three that contributed to growing the new grain.

There are challenges to implement the critical events. First, the general algorithms for critical events fail when a two boundary facet is involved in the event. And this case should

be taken care of separately. In addition we have the difficulty of tuning parameters for each critical event, i.e. loss of grain, loss of surface and loss of triple lines. These parameters determine whether a given grain, facet or triple line is considered for deletion. The precise value of such parameters is not expected to influence statistical properties of the system, but configuration may be altered slightly with different choice.

0.4 Numerical Results

We illustrate our method using some numerical results in two and, briefly, in three dimensions. For simplicity and ease of comparison, we confine ourselves to the case where the energy density $\sigma = const.$ and the mobility $\mu = 1$. In two dimensions, we may typically begin from a 25,000 to 50,000 Voronoi-type initial configuration. We are able to verify these diagnostics: the average area grows linearly with time, the Mullins-von Neumann $n - 6$- rule holds for individual grains (not undergoing a critical event), and a 'round' grain shrinks inversely to its radius at the proper rate (to second order in spatial discretization.) For the general large scale simulation, we may plot relative area histograms, as in Fig. (0.4). below. These show a transient phase and then remarkable self-similarity. More details are available in [18].

An important feature of the our technique is the ability to simulate with anisotropic energy densities $\sigma = \sigma(n, \alpha)$, that is, energies which depend both on the normal to the curve n and the lattice misorientation α. Lack of space prevents us from discussing this, but a glimpse of the new and interesting phenomena we are able to investigate is given in [31].

In three dimensions we are presently implementing large scale simulations. On average, grains with a large number of facets, say greater than 14, grow and grains with few facets shrink. An example of a critical event is portrayed below.

0.5 Conclusion

In this paper we have presented a consistent variational approach to the mesoscale simulation of grain growth in three dimensions. We have presented results for a 'bamboo structure', a system with constant energy and mobility. The method accurately computes curvature driven growth with the Herring Condition imposed at triple junctions. The issues we had to resolve to accomplish this include the correct discretization scheme and the treatment of critical events.

An important feature of the mesoscale approach is that it respects the thermodynamic formulation given by Mullins and Herring. The reduced dimensionality of its data structure permits simulation of large scale systems, indeed, systems sufficiently large that we may inquire about their statistics. We found that the statistics produced by our simulation are very robust.

Future work can exploit this method to investigate interface dominated properties, for example, questions about anisotropy, texture, and abnormal grain growth, as mentioned in the Introduction. As a first project, we are exploring the role of anisotropy.

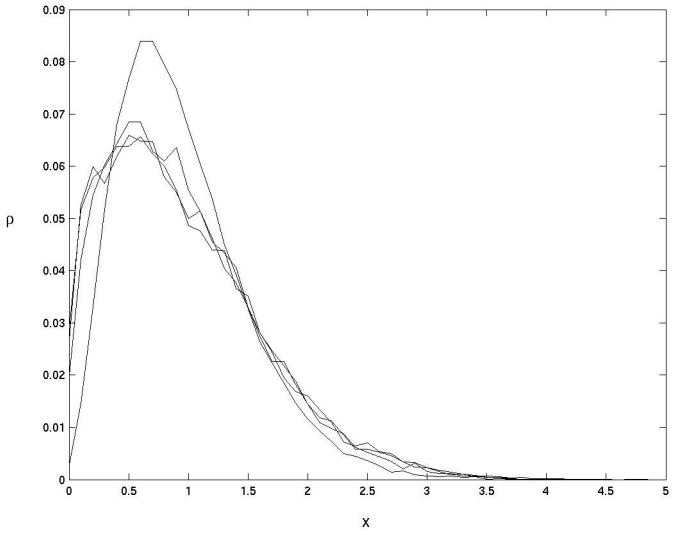

Figure 4: The relative density ρ plotted against relative area x = area/(average area) at initial time (plot with highest maximum), time = 5 (plot with next highest maximum), and time = 10 and time = 15, which are essentially the same.

Other statistics may be collected as well, for example, the fraction of grains with a given number of sides, illustrated in Figure 2 at a time step when the relative area histogram is stationary.

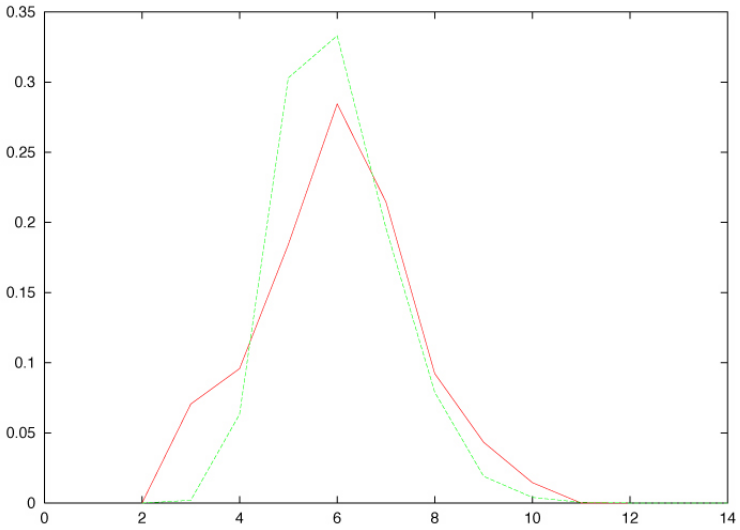

Figure 5: The population of grains sorted by number of edges during evolution (higher curve) and at the stationary position of the relative area histogram (lower curve). Note the peak at 6 sides

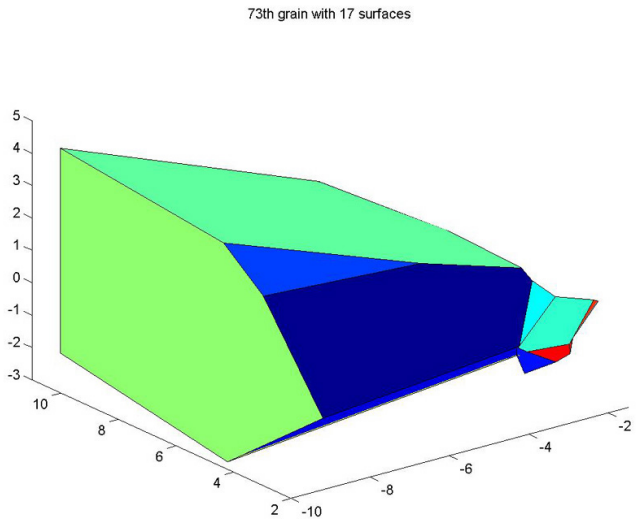

Figure 6: Grain 73 has grown while grain 57 has shrunk. The figure shows the loss of grain 57 into grain 73. Faces are rendered as polyhedra but are, in fact, curvelinear.

Bibliography

[1] Adams, B.L. et al *Extracting grain boundary and surface energy from measurement of triple junction geometry*, Interface Science, 7, pp. 321-338, 1999.

[2] Anderson, M.P., Srolovitz D.J. et al *Computer Simulation of Grain Growth I. Kinetics*, Acta Metallurgica, 32(5), pp. 783-791, 1985.

[3] Anderson, M.P., Grest G., et al *Computer Simulation of Grain Growth in Three Dismensions*, Phil. Mag. B 59(3), pp. 293-329, 1989.

[4] J. Bragard, A. Karma, H.Y. H. Lee, M. Plapp *Linking Phase-Field and Atomistic Simulations to Model Dendritic Solidification in Highly Undercooled Melts*, Interface Science, 10 (2-3), pp. 121-136, 2002.

[5] Chen, L.Q., *A Novel Computer Simulation Technique for Modeling Grain Growth*, Scripta Metallurgica et Materialia, 32(1), pp. 115-120, 1995.

[6] F. Cleri, S. R. Phillpot, D. Wolf *Atomistic Simulations of Integranular Fracture in Symmetric-Tilt Grain Boundaries*, Interface Science, 7(1), pp. 45-55, 1999.

[7] Demirel, M.C., Kuprat, A., George, D.C., Straub, G., and Rollett, A.D. *Linking experimental characterization and computational modeling of grain growth in Al-foil*, Interface Science, 10, pp. 137-142, 2002.

[8] Fradkov, V.E., M.E. Glicksman, et al *Topological Events in Two-dimensional Grain Growth*, Acta Metall. Mater., 42(8), pp. 2719-2727, 1994.

[9] Fradkov, V.E., Udler D. *Two Dimensional Normal Grain Growth: Topological Aspects*, Advances in Physics, 43(6), pp. 739-789, 1994.

[10] Fradkov, V.E.*Main Regularities of 2-D Normal Growth*, Material Science Forum, 94-96, pp. 269-274, 1992.

[11] H.J. Frost, C.V. Thompson, D.T Walton *Simulation of Thin Film Grain Structures: I. Grain Growth Stagnation*, Acta Metallurgica et Materiala, 38, pp. 1455, 1990.

[12] Frost, H.J. and Thompson, C.V., et al. *A Two Dimensional Computer Simulation of Capillarity-driven Grain Growth: Preliminary Results*, Scripta Met., 22, pp. 62-70, 1988.

[13] Haslam A.J., Phillpot, et al *Mechanism of Grain Growth in Nanocrystalline for Metals by Molecular Dynamic Simulation*, Mater. Sci. Eng. A, to appear.

[14] Herring, C., Chapter 8 in The Physics of Powder Metallurgy, W. E. Kingston, ed., MacGraw-Hill, New-York, p. 143, 1951.

[15] Herring, C., *The Use of Classical Macroscopic Concepts in Surface Energy Problems*, in Structure and properties of Solid Surfaces, (Gomer,R. and Simth, C., eds) U.Chicago Press, Chicago, 1952.

[16] Keblinski. P., Wolf. D, Phillpot, S., R. *Molecular-Dynamics Simulations of Grain Boundary Diffusion Creep*, Interface Science, 6, p. 205-212, 1998.

[17] Kinderlehrer, D. and Liu, C. *Evolution of Grain Boundaries*, Math. Models and Meth. Appl. Math. 11.4, pp. 713-729, 2001.

[18] Kinderlehrer D., Livshits I., Ta'asan S., *A variational approach to modeling and simulation of grain growth*, submitted

[19] Kinderlehrer D., Livshits I., Ta'asan S., *On Some Stochastic Models for Grain Growth*, in preparation.

[20] Kinderlehrer, D., Manolache, F., Livshits, I., Rollett, A., and Ta'asan, S. *An approach to the mesoscale simulation of grain growth*, Mat. Res. Soc. Proc. 652, (Aindow et al., eds), 2001, Y.1.5

[21] Kobayashi, R., Warren, J.A., Carter, W.C. *Vector-Valued Phase Field Model for Crystallization and Grain Boundary Formation*, Physica D, 119 (3-4), pp. 415-423, 1998.

[22] Krill, C. E. and Chen, L. Q. *Computer Simulation of 3-D Grain Growth Using a Phase-field Model*, Acta Materialia, 50, pp. 3057-3073, 2002.

[23] Kuprat, A., *Modeling Microstructure Evolution Using Gradient-Weighted Finite Elements*, SIAM J. Sci. Comput, 22(2), pp. 535-560, 2000.

[24] Mehnert, K., Klimanek, P, *Monte Carlo Simulation of Grain Growth in Textured Metals*, Scripta Materialia, 30(6), pp. 699-704, 1996

[25] M.I. Mendelev, D.J. Srolovitz *Co-Segregation Effects on Boundary Migration* , Interface Science 10, pp. 191-199, 2002.

[26] M.Morhac, E.Morhacova, *Monte Carlo Simulation Algorithms of Grain Growth in Polycrystalline Materials*, Cryst.Res. Technol., 35(1), pp. 117-128, 2000.

[27] Mullins, W.W. *Two-dimensional Motion of Idealized Grain Boundaries*, J. Appl. Phys., 27, pp. 900-904, 1956.

[28] Mullins, W.W. *Solid Surface Morphologies Governed by Capillarity*, Metal Surfaces: Structure, Energetics, and Kinetics, ASM, Cleveland, pp. 17-66, 1963.

[29] S.R. Phillpot, P. Keblinski, D. Wolf, F. Cleri *Synthesis and Characterization of a Polycrystalline Ionic Thin Film by Large-Scale Molecular-Dynamics Simulation*, Interface Science, 7 (1), pp. 15-31, 1999.

[30] Schoenfelder, B., Wolf. D, Phillpot, S., R., *Molecular-Dynamics Method for Simulation of Grain Boundary Migration*, Interface Science, 5, pp. 245-262, 1997.

[31] Ta'asan, S., P. Yu, I. Livshits, D. Kinderlehrer, and J. Lee, *Multiscale modeling and simulation of grain boundary evolution* AIAA-2003-1611, 44th AIAA/ASME/ASCE/AHS Structures, Structural Dynamics, and Materials Conference Norfolk , VA

[32] Thompson, C. V., *Grain growth and evolution of other cellular structures*, Solid State Phys., 55, 269-314, 2001

[33] M. Upmanyu, R.W. Smith, D.J. Srolovitz *Atomistic Simulation of Curvature Driven Grain Boundary Migration*, Interface Science, 6(1-2), 1998.

[34] M. Upmanyu, D.J. Srolovitz, L.S. Shvindlerman, G. Gottstein *Triple Junction Mobility: A Molecular Dynamics Study*, Interface Science, 7 (3-4), 1999.

[35] M. Upmanyu, D. J. Srolovitz, L. S. Shvindlerman and G. Gottstein *Misorientation Dependence of Intrinistic Grain Boundary Mobility: Simulation and Experiment*, Acta Mater., 47, pp. 3901-3914, 1999.

[36] M. Upmanyu, G.N. Hassold, A. Kazaryan, E.A. Holm, Y. Wang, B. Patton, D.J. Srolovitz *Boundary Mobility and Energy Anisotropy Effects on Microstructural Evolution During Grain Growth* , Interface Science, 10, pp. 201-216, 2002.

[37] Weaire, D., J. P. Kermode *Computer simulation of a two-dimensional soap froth I. Method and motivation*, Phil. Mag. B 48(3), pp. 245-259, 1983.

[38] Weaire, D, J. P. Kermode *Computer simulation of a two-dimensional soap froth II. Analysis of results*, Phil. Mag. B 50(3), pp. 379-395, 1984.

[39] D. Weygand, Y. Brechet, J. Lepinoux *Mechanisms and Kinetics of Recrystallisation: A Two Dimensional Vertex Dynamics Simulation*, Interface Science, 9(3-4), pp. 311-317, 2001.